This document is confidential and is proprietary to the American Chemical Society and its authors. Do not copy or disclose without written permission. If you have received this item in error, notify the sender and delete all copies.

Slow Auger Relaxation in HgTe Colloidal Quantum Dots

Journal:	The Journal of Physical Chemistry Letters	
Manuscript ID	jz-2018-00750n.R2	
Manuscript Type:	Letter	
Date Submitted by the Author:	11-Apr-2018	
Complete List of Authors:	Melnychuk, Christopher; University of Chicago Division of the Physical Sciences, Chemistry Guyot-Sionnest, Philippe; university of chicago, james franck institute	

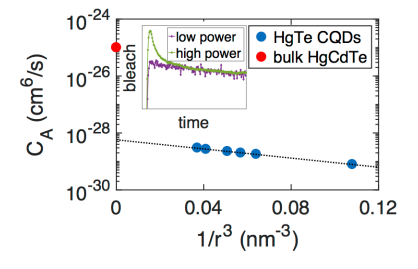


Slow Auger Relaxation in HgTe Colloidal Quantum Dots

Christopher Melnychuk and Philippe Guyot-Sionnest

James Franck Institute, The University of Chicago, 929 East 57th Street, Chicago, Illinois 60637

The biexciton lifetimes in HgTe colloidal quantum dots are measured as a function of particle size. Samples produced by two synthetic methods, leading to partially aggregated or well-dispersed particles, exhibit markedly different dynamics. The relaxation characteristics of partially aggregated HgTe inhibit reliable determinations of the Auger lifetime. In well-dispersed HgTe quantum dots, the biexciton lifetime increases approximately linearly with particle volume, confirming trends observed in other systems. The extracted Auger coefficient is three orders of magnitude smaller than for bulk HgCdTe materials with similar energy gaps. We discuss these findings in the context of understanding Auger recombination in quantum-confined systems, and their relevance to mid-infrared optoelectronic devices based on HgTe colloidal quantum dots.



At high carrier densities, the dominant mode of energy loss in semiconductors is Auger relaxation. In this process, electrons and holes recombine non-radiatively by transferring the gap energy to a third carrier that rapidly thermalizes. Auger processes are very relevant to the performance of semiconductor devices, including lasers, high power light emitting diodes, and detectors. In particular, they are the main reason why infrared semiconductor detectors, such as InSb and HgCdTe, must be operated at cryogenic temperatures. Auger relaxation in these small-gap semiconductors is a direct process modeled accurately by the Coulomb interactions between carriers under total momentum conservation. In contrast, for wide-gap semiconductors such as InGaN, the theoretical direct process is orders of magnitude too slow compared to experiment. Auger relaxation in these materials is instead better described as an indirect process involving phonons. As a general trend, the Auger relaxation rates in bulk semiconductors decrease by many orders of magnitude as the energy gap increases.

Auger relaxation in quantum dots happens as soon as one or more carriers interact with an exciton, and it is easily observed as a shortened exciton lifetime under strong excitation. The first report of such behavior in 1987 showed sub-nanosecond Auger lifetimes for CdSe_xS_{1-x} nanoparticles in glass.⁴ Subsequent investigations of Auger relaxation in colloidal quantum dots led to the striking observation that many different materials displayed similar biexciton lifetimes despite vast differences in their bulk Auger rates. In particular, a comparative study of Auger lifetimes for PbSe, InAs, CdSe, and Ge colloidal quantum dots showed a "universal" linear scaling of the biexciton lifetime with particle volume and a weak effect of the material.⁵ In addition to colloidal

nanoparticles, epitaxial quantum well structures display a comparable dissimilarity between bulk and nanoscale Auger rates.⁶

Relaxation of momentum conservation has been qualitatively proposed to account for these observations, ^{5,7} but there is no quantitative theory that explains the similar biexciton lifetimes in quantum dots of such different materials, or their differences from those in the bulk. The unexplained differences between bulk and nanoscale Auger lifetimes motivate experiments on materials with even faster Auger rates in the bulk, such as small-gap materials including the semimetal HgTe. The Auger lifetimes in HgTe CQDs are also of interest as they are investigated for low-cost infrared detectors and light sources. ^{8–12} To date, there are two reports of an approximately 50 ps Auger lifetime in small HgTe particles. ^{13,14} Here, we describe a more extended study of the Auger lifetime size-dependence in HgTe quantum dots, made possible by recent synthetic methods.

In this work, we employed the method of transient bleaching in the mid-infrared. A home-built Nd:YLF regenerative amplifier producing 10 ps, 1053 nm pulses at 1 kHz was used to generate pulses tunable from $1.4-4.5~\mu m$ by type II parametric down-conversion. The idler waves were selected as probes by a Ge plate at Brewster's angle, and 1053 nm pulses pumped the sample after a variable optical delay. Probe pulses were attenuated by NiCr-CaF₂ neutral density filters to below $22~\mu J/cm^2$ at the sample, and pump pulses were attenuated by a variable neutral density filter. The pump and probe beam waists at the sample were respectively 1.3 and 0.12 mm.

Partially aggregated HgTe quantum dots were prepared by a variant of the synthesis reported by Keuleyan and co-workers.¹⁵ Briefly, 30 mg of HgCl₂ was dissolved in 4 mL of oleylamine by stirring at 100 °C for one hour in a N₂ glove box. The solution

was then cooled to the desired reaction temperature, determined by the target particle size, and reacted with 130 µL of injected 1M trioctylphosphine telluride for 40 minutes while stirring. After reaction quenching, the particles were cleaned and capped with 1dodecanethiol ligands. Well-dispersed particles were synthesized in a N₂ glove box following Shen et al. 16 HgCl₂ was dissolved in oleylamine as above, cooled to the desired reaction temperature, and reacted with 15 µL of injected bis(trimethylsilyl)telluride for five minutes while stirring. After reaction quenching, the particles were cleaned and left with oleylamine as the surface ligand. All samples were dispersed in tetrachloroethylene for measurements and placed either in a glass cuvette with 1 mm path length or a cell consisting of two CaF₂ windows and a 1.3 mm PTFE spacer. Absorbance values at the band edge were typically between 0.09 and 0.15. Samples were not stirred or otherwise agitated during measurements. We determined that photopumping did not appreciably alter the samples by confirming that photoluminescence intensities and lineshapes were effectively identical before and after measurements, negative-time absorption did not change before and after data collection sessions, and low-fluence transient data were identical before and after high-fluence measurements.

Figure 1a shows transient bleaching data for partially aggregated HgTe nanoparticles. Auger relaxation is apparent as the faster early-time bleach decay appearing with increasing optical fluence. As done previously on similar particles, one may extract an Auger rate. However, figure 1a shows that the long-time bleach magnitude saturates well below half the band-edge absorbance A₀ with increasing excitation. This implies that Auger is possible at much less than one excitation per dot, in conflict with the typical picture of the process. We rationalize this observation by

invoking the partially aggregated nature of the solutions studied, which is apparent in TEM images. These transient data also suggest that inter-dot electron/hole transfer within aggregates is fast enough to allow biexciton relaxation with less than one exciton per quantum dot. Although investigating the dynamics of Auger relaxation in partially aggregated HgTe CQDs may be of interest, reliable measurements of the intrinsic rates require well-dispersed particles. This is provided by a recent synthetic method for welldispersed HgTe CQDs of tunable size. 16 Representative data for such nanocrystals are shown in figure 1b. In these samples, the magnitude of the long-time bleach increases with pump fluence as one expects from an increasing population of singly excited particles. At a low pump fluence of 26 µJ/cm², we observe almost no relaxation on the timescale of the measurement. Larger optical fluence induces a fast relaxation component while the slow relaxation rate remains unchanged. At high fluence, the long-time bleach is approximately $A_0/2$ and the early-time bleach is almost 80 % of A_0 . This behavior agrees well with similar Auger measurements in other systems, 17-19 and we therefore assign the fast relaxation to Auger recombination.

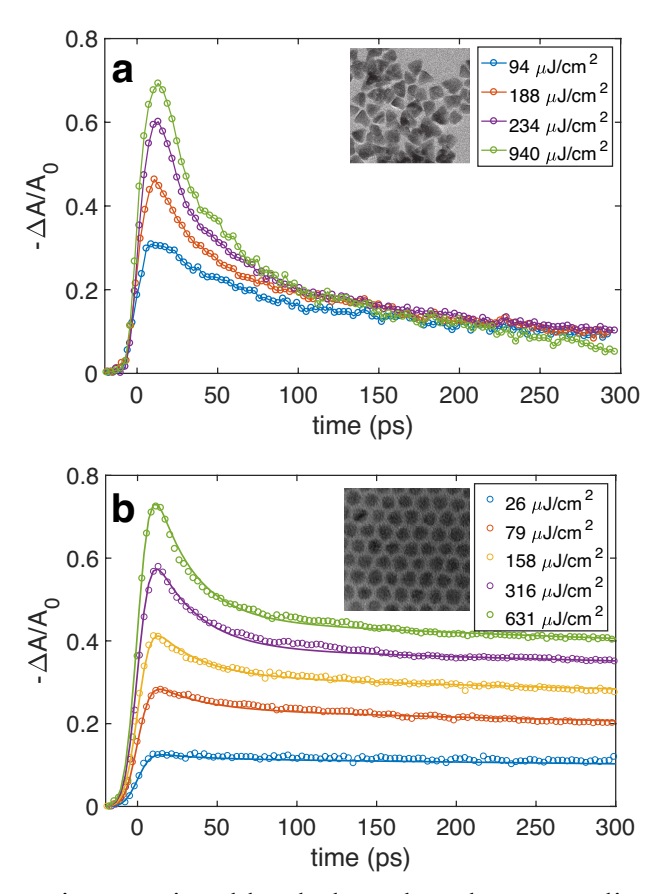


Figure 1: Representative transient bleach data plotted as normalized absorbance changes $\Delta A/A_0$ for (a) aggregated particles (3950 cm⁻¹ band edge) and (b) non-aggregated particles (4200 cm⁻¹ band edge) at various pump fluences. The band-edge absorbances, A_0 , were 0.18 (a) and 0.14 (b). Representative TEM images for the particle types are inset. Curves through the data in (b) are convolutions described in the text.

The data in figure 1b are described well by the convolution of a Gaussian function (15 ps full width at half maximum) and a biexponential decay of the form $a_1e^{-t/\tau_X}+a_2e^{-t/\tau_{BX}}$. Fitting gives $\tau_X=3100$ ps for the exciton lifetime and $\tau_{BX}=30$ ps for the biexciton lifetime. As we discuss later, this biexciton lifetime is much longer than expected based on the Auger coefficient of bulk HgTe. One concern, then, is that the 10 ps pulses used in this experiment do not resolve a much faster Auger relaxation. Although this is unlikely given the well-resolved power-dependent decay, we further rule this out through a quantitative analysis of the bleach amplitudes. Figure 2 shows how $1-a_1$ and a_2 vary with pump energy.

To model these amplitudes as a function of the pump energy, we first determined the absorption cross section at the pump wavelength of 1053 nm, σ_p . This begins with the calculation of the nanocrystal cross section at 415 nm, σ_{415}^{NC} , using the particle volume and the reported absorption cross section per Hg atom in an HgTe nanoparticle at 415 nm, $\sigma_{415}^{Hg}=2.6\pm0.4\times10^{-17}~{\rm cm}^2.^{20}$ The measured relative absorbances at 415 nm and 1053 nm then give σ_p via $\sigma_p = \frac{A_{1053}^{NC}}{A_{415}^{NC}} \times \sigma_{415}^{NC}$. For example, a dot with an interband transition at 4200 cm⁻¹ has $\sigma_p=1.9\pm0.3\times10^{-15}$ cm², with the uncertainty due to σ_{415}^{Hg} . With the particle concentration c and the incident photon fluence I_0 , the average number of excitations per particle is calculated as a function of position z in the sample cell by $\sigma_p I_0 \, e^{-\sigma_p cz}$. A Poisson distribution of excitation levels 21 then gives the local concentration of quantum dots in the ground state, c_0 , with one exciton, c_1 , and two or more excitons, c_2 , with $c_0 + c_1 + c_2 = c$. Due to the doubly degenerate nature of the lowest electron state 1S_e, dots with one exciton are bleached by half ($\Delta A = -A_0/2$), and dots with two or more excitons do not absorb at the band edge ($\Delta A = -A_0$). Before the pump pulse, the absorbance at the band edge is $A_0 = \frac{1}{\ln{(10)}} \int \sigma c \, dz$. Right after the pulse, the absorbance is reduced to $A_{early} = \frac{1}{\ln{(10)}} \int \sigma{(c_0 + \frac{c_1}{2})} dz$. At long time, when the multiple excitons relax to single-exciton states, the absorbance recovers to A_{late} = $\frac{1}{\ln{(10)}}\int\sigma\left(c_0+\frac{c_1}{2}+\frac{c_2}{2}\right)dz \ . \quad \text{The ratio } A_{late}/A_0 \ \text{is } 1-\frac{\langle c_1+c_2\rangle}{c}=1-a_1, \text{ where } \langle -\rangle$ denotes a spatial average across the sample cell thickness. As shown in figure 2, $1-\alpha_1$ decreases from one at low power to one-half at high power in both simulation and experiment. The ratio $(A_{late} - A_{early})/A_0 = \frac{\langle c_2 \rangle}{c} = a_2$, and represents the early time bleach due to doubly excited quantum dots. This increases from zero to one-half as the pump power increases in both simulation and experiment. The good overall agreement between simulation and experiment further supports our assignment of the fluence-dependent bleach decay to Auger relaxation and allows us to rule out the presence of faster, unresolved Auger processes.

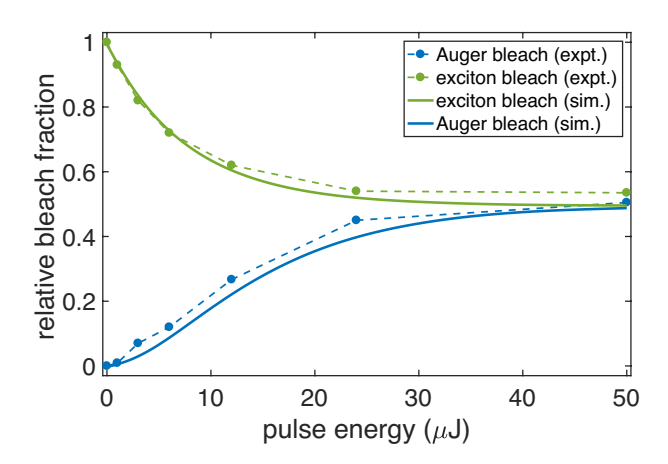


Figure 2: Experimental (points) and simulated (solid lines) bleaching ratios, giving the relative proportions of Auger (blue) and single-exciton (green) contributions to the bleach. Experimental data were taken from the dataset shown in figure 1b. Simulations used $\sigma_p = 1.5 \times 10^{-15} \text{ cm}^2$.

We obtained transient bleach data for particles with band edges ranging from 2500 cm^{-1} to 4700 cm^{-1} , and the results are shown in table 1 and figure 3. The exciton lifetimes generally shorten with increasing particle size, consistent with decreased photoluminescence efficiencies as the gap approaches the mid-infrared. In contrast, the biexciton lifetimes consistently lengthen with increasing particle size. We find the biexciton lifetime to be reasonably linear in r^3 , where r is the particle radius, in agreement with the findings of Robel and co-workers. Fitting the data to $\tau_{BX} = pr^3$ gives a scaling coefficient p of 1.9 ps/nm³ (figure 3). Also shown in figure 3 is the

corresponding curve for CdSe, for which $p = 5.5 \text{ ps/nm}^{3.5}$ This indicates that for the same particle size, biexciton lifetimes are only three times shorter in HgTe than in CdSe. This result is remarkable, considering that the Auger rates differ by many orders of magnitude in the respective bulk materials.^{1,5}

PL (cm ⁻¹)	radius (nm)	biexciton lifetime (ps)	exciton lifetime (ps)
2500 (800)	4.4 (5.0, 3.8)	> 80	790
3600 (600)	3.0 (3.5, 2.6)	50 (56, 45)	1300
3750 (800)	2.9 (3.3, 2.5)	46 (50, 39)	3000
3950 (800)	2.7 (3.1, 2.4)	37 (40, 33)	7500
4050 (800)	2.6 (3.0, 2.3)	34 (39, 31)	3000
4200 (700)	2.5 (2.7, 2.3)	30 (33, 28)	3100
4700 (900)	2.1 (2.4, 1.8)	24 (28, 19)	5000

Table 1: Photoluminescence (PL) peaks with full-width half-maxima (FWHM) in parentheses. Particle radii were estimated by fitting PL-diameter data, ¹⁶ giving $r = 10.225 \exp(-3.38m \times 10^{-4})$ for the PL value m (cm⁻¹) and particle radius r (nm). The bounds on these radii correspond to PL FWHM. Biexciton lifetimes with limits reflecting 95% confidence intervals were obtained by fitting the data to biexponential decays. Exciton lifetimes were also obtained from the fits.

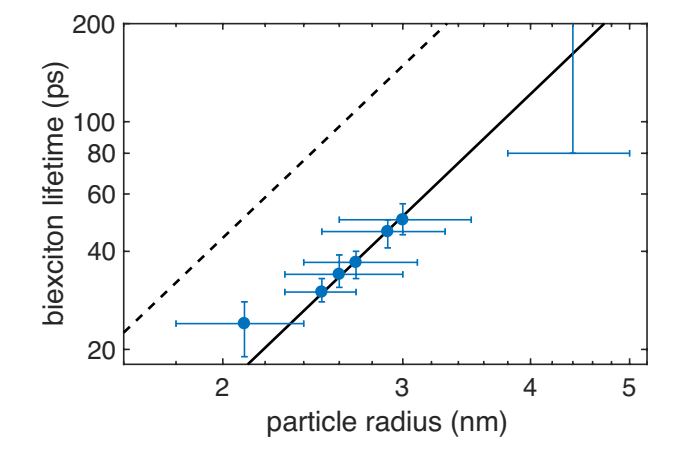


Figure 3: Size-dependence of the biexciton lifetime. Bounds are those from table 1. Horizontal error bars reflect the particle size distributions (FWHM), the average sizes being known with accuracy comparable to the symbol size. The solid line is the r^3 fit discussed in the text, and the dashed line is the corresponding curve for CdSe quantum dots. The rightmost error bars reflect our estimated lower bound for the biexciton lifetime of a particle with a 4.4 nm radius, as discussed in the text.

When performing measurements on larger particles, we could no longer obtain fluence-dependent decay curves. Figure 4 shows data for a sample with a photoluminescence peak at 2500 cm⁻¹. The bleach increases with pump power as seen in 4a, but figure 4b clearly shows that the relative amplitudes of the fast and slow decays do not depend on pump fluence. The maximum bleach exceeds half the sample optical density, supporting the absence of an Auger relaxation much faster than the pulse resolution. The curves are well characterized by two unchanged decay components of 22 and 790 ps, both attributable to non-radiative pathways. It could be the case that these reflect two classes of particle, one of which lies closer to the 2900 cm⁻¹ region with a known faster non-radiative relaxation via coupling to surface ligand C-H vibrations.¹³ Although partial n-doping in small-gap materials and thus negative trion decay is possible, it is unlikely in this sample because the photogeneration of trions would still produce decay curves that change with pump power.²² We conclude that the biexciton relaxation is not resolved in large HgTe quantum dots because it is too slow, and possibly masked by the exciton relaxation. We estimate a lower bound for the Auger lifetime by fitting the data to a triple exponential decay, and such a fit implies a biexciton Auger lifetime longer than 80 ps. This is consistent with the r^3 fit in figure 3, and would indeed be difficult to observe on the timescale of our measurements given the presence of other relaxation processes.

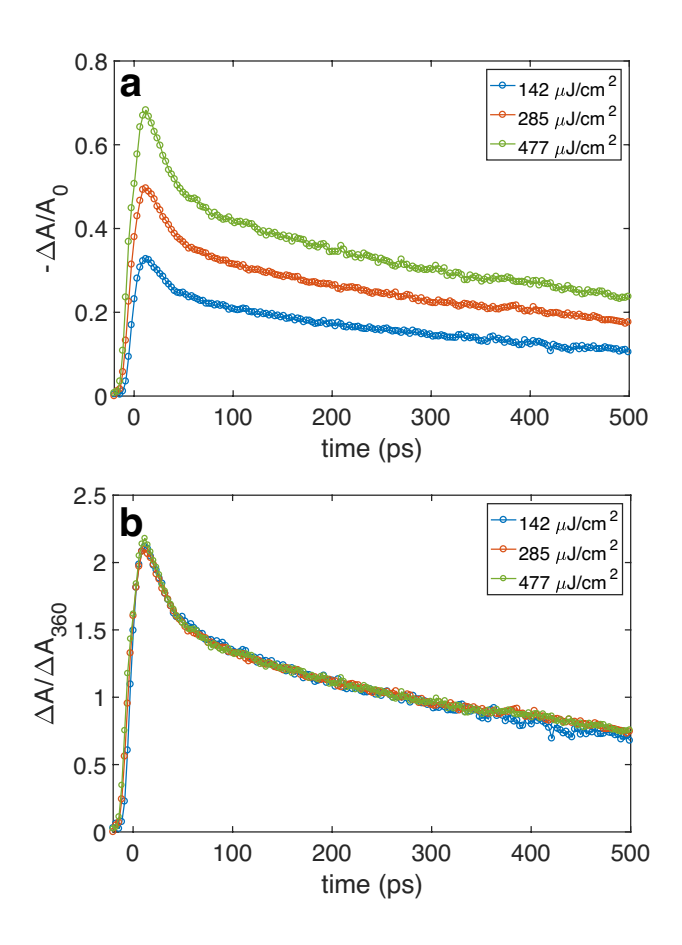


Figure 4: Transient data for well-dispersed particles with a 2500 cm⁻¹ band edge (a), and the same three curves normalized to their magnitudes at 360 ps (b). A_0 was 0.19.

We now compare the Auger relaxation rates in HgTe quantum dots to those of bulk Hg_{1-x}Cd_xTe with similar gap. In bulk semiconductors, the Auger carrier loss is cubic in the carrier density and characterized by Auger coefficients C_A associated with different possible combinations of electrons and holes. In nanoparticles, C_A relates the biexciton lifetime τ_{BX} to the particle volume V by $C_A = \frac{V^2}{8\tau_{BX}}$. For a variety of quantum dot materials, C_A has been observed to scale as $C_A = \gamma r^3$. The data in figure 3 correspond to

 $\gamma = 1.2 \times 10^{-9}$ cm³/s and Auger coefficients from 0.7×10^{-29} cm⁶/s at 2.1 nm radius to 3×10^{-29} cm⁶/s at 3.0 nm radius. Using the value of γ and extrapolating to 0.12 eV bandgap ($r \approx 7.2$ nm) gives $C_A = 4 \times 10^{-28}$ cm⁶/s for an HgTe nanoparticle. This is three orders of magnitude smaller than for bulk HgCdTe with the same gap, 10^{-25} cm⁶/s.¹ We therefore find that Auger relaxation is very strongly suppressed in HgTe CQDs relative to bulk HgCdTe. For applications in mid-infrared detection, the slower Auger relaxation is an intrinsic advantage of the HgTe colloidal quantum dots that should allow higher operating temperatures than bulk HgCdTe.

In summary, we presented an experimental study of Auger relaxation in HgTe colloidal quantum dots. Time-resolved bleaching experiments revealed conspicuously different relaxation dynamics between aggregated and non-aggregated HgTe, and we concluded that aggregated particles are not amenable to a quantitative study of Auger rates by transient bleaching. Measurements on well-dispersed particles allowed us to determine the Auger lifetime as a function of particle size. The magnitude and scaling of the Auger lifetime agree well with trends observed in other colloidal quantum dot systems, and our measurements extend these trends to the mid-infrared. We showed that Auger relaxation in HgTe nanoparticles is suppressed relative to bulk HgCdTe by three orders of magnitude. The much slower Auger relaxation in HgTe colloidal quantum dots versus bulk infrared materials is a fundamental benefit for infrared detection and lasing.

Acknowledgements

C. M. acknowledges Guohua Shen for providing helpful advice on the preparation of well-dispersed HgTe nanoparticles. The instrumentation was developed with primary funding from the Defense Advanced Research Projects Agency (DARPA) as a subcontract to Voxtel, Inc. for the Wired program. C. M. was supported by NSF DMR-1708378. This work was partially supported by the University of Chicago Materials Research Science and Engineering Center, which is funded by the National Science Foundation under award number DMR-1420709.

References

- (1) Landsberg, P. T. *Recombination in Semiconductors*; Cambridge University Press: Cambridge, U. K.; 1991.
- (2) Rogalski, A.; HgCdTe infrared detector material: history, status and outlook. *Reports Prog. Phys.* **2005**, *68*, 2267–2336.
- (3) Kioupakis, E.; Rinke, P.; Delaney, K. T.; Van De Walle, C. G.; Indirect Auger recombination as a cause of efficiency droop in nitride light-emitting diodes. *Appl. Phys. Lett.* **2011**, *98*, 2009–2012.
- (4) Roussignol, P; Kull, M.; Ricard, D.; de Rougemont, F.; Frey, R.; Flytzanis, C.; Time-resolved direct observation of Auger recombination in semiconductor-doped glasses. *Appl. Phys. Lett.* **1987**, *51*, 1882–1884.
- (5) Robel, I.; Gresback, R.; Kortshagen, U.; Schaller, R. D; Klimov, V. I.; Universal size-dependent trend in auger recombination in direct-gap and indirect-gap semiconductor nanocrystals. *Phys. Rev. Lett.* **2009**, *102*, 177404.
- (6) Meyer, J. R.; Felix, C.L.; Bewley, W. W.; Vurgaftman, I.; Aifer, E. H.; Olafsen, L. J.; Lindle, J. R.; Hoffman, C. A.; Yang, M. -J.; Bennett, B. R.; et al. Auger coefficients in type-II InAs/Ga_{1-x}In_xSb quantum wells. *Appl. Phys. Lett.* 1998, 73, 2857–2859.
- (7) Pietryga, J. M.; Park, Y. -S.; Lim, J.; Fidler, A. F.; Bae, W. K.; Brovelli, S.; Klimov, V. I.; Spectroscopic and device aspects of nanocrystal quantum dots. *Chem. Rev.* **2016**, *116*, 10513–10622.
- (8) Lhuillier, E.; Keuleyan, S.; Guyot-Sionnest, P.; Colloidal quantum dots for mid-IR applications. *Infrared Phys. Technol.* **2013**, *59*, 133–136.

- (9) Keuleyan, S.; Lhuillier, E.; Brajuskovic, V.; Guyot-Sionnest, P.; Mid-infrared HgTe colloidal quantum dot photodetectors. *Nat. Photonics* **2011**, *5*, 489–493.
- (10) Kershaw, S. V.; Susha, A. S; Rogach, A. L.; Narrow bandgap colloidal metal chalcogenide quantum dots: synthetic methods, heterostructures, assemblies, electronic and infrared optical properties. *Chem. Soc. Rev.* **2013**, *42*, 3033–3087.
- (11) Lhuillier, E.; Guyot-Sionnest, P.; Recent Progresses in Mid Infrared Nanocrystal based Optoelectronics. *IEEE J. Sel. Top. Quantum Electron.* **2017**, *23*, 6000208.
- (12) Geiregat, P.; Houtepen, A. J.; Sagar, L. K.; Infante, I.; Zapata, F.; Grigel, V.; Allan, G.; Delerue, C.; Van Thourhout, D.; Hens, Z.; Continuous-wave infrared optical gain and amplified spontaneous emission at ultralow threshold by colloidal HgTe quantum dots. *Nat. Mater.* **2018**, *17*, 35–42.
- (13) Keuleyan, S.; Kohler, J; Guyot-Sionnest, P; Photoluminescence of mid-infrared HgTe colloidal quantum dots. *J. Phys. Chem. C* **2014**, *118*, 2749–2753.
- (14) Al-Otaify, A.; Kershaw, S. V.; Gupta, S.; Rogach, A. L.; Allan, G.; Delerue, C.; Binks, D. J.; Multiple exciton generation and ultrafast exciton dynamics in HgTe colloidal quantum dots. *Phys. Chem. Chem. Phys.* **2013**, *15*, 16864–16873.
- (15) Keuleyan, S.; Lhuillier, E; Guyot-Sionnest, P.; Synthesis of colloidal HgTe quantum dots for narrow mid-IR emission and detection. *J. Am. Chem. Soc.* **2011**, *133*, 16422–16424.
- (16) Shen, G.; Chen, M.; Guyot-Sionnest, P.; Synthesis of Nonaggregating HgTe Colloidal Quantum Dots and the Emergence of Air-Stable n-Doping. *J. Phys. Chem. Lett.* **2017**, *8*, 2224–2228.
- (17) Klimov, V. I.; Mikhailovsky, A. A.; Xu, S.; Malko, A.; Hollingsworth, J. A.;

- Leatherdale, C. A.; Eisler, H.-J.; Bawendi, M. G.; Optical Gain and Stimulated Emission in Nanocrystal Quantum Dots. *Science*. **2000**, *290*, 314–317.
- (18) Kobayashi, Y.; Nishimura, T.; Yamaguchi, H.; Tamai, N.; Effect of Surface Defects on Auger Recombination in Colloidal CdS Quantum Dots. *J. Phys. Chem. Lett.* 2011, 2, 1051–1055.
- (19) Pandey, A.; Guyot-Sionnest, P.; Multicarrier recombination in colloidal quantum dots. *J. Chem. Phys.* **2007**, *127*, 111104.
- (20) Lhuillier, E.; Keuleyan, S; Guyot-Sionnest, P.; Optical properties of HgTe colloidal quantum dots. *Nanotechnology* **2012**, *23*, 175705.
- (21) Klimov, V. I.; McGuire, J. A.; Schaller, R. D.; Rupasov, V. I.; Scaling of multiexciton lifetimes in semiconductor nanocrystals. *Phys. Rev. B Condens. Matter Mater. Phys.* **2008**, *77*, 1–12.
- (22) Jha, P. P.; Guyot-Sionnest, P.; Trion decay in colloidal quantum dots. *ACS Nano* **2009**, *3*, 1011–1015.

